



Title	Quantum-classical crossover for biaxial antiferromagnetic particles with a magnetic field along the hard axis
Author(s)	Zhou, B; Tao, R; Shen, SQ
Citation	Physical Review B - Condensed Matter And Materials Physics, 2004, v. 70 n. 1, p. 012409-1-012409-4
Issued Date	2004
URL	http://hdl.handle.net/10722/43457
Rights	Creative Commons: Attribution 3.0 Hong Kong License

Quantum-classical crossover for biaxial antiferromagnetic particles with a magnetic field along the hard axis

Bin Zhou,^{1,2,3} Ruibao Tao,¹ and Shun-Qing Shen²¹*Department of Physics, Fudan University, Shanghai 200433, China*²*Department of Physics, The University of Hong Kong, Hong Kong, China*³*Department of Physics, Hubei University, Wuhan 430062, China*

(Received 16 December 2003; revised manuscript received 8 March 2004; published 28 July 2004)

Quantum-classical crossover of the escape rate is studied for biaxial antiferromagnetic particles with a magnetic field along the hard axis. The phase boundary line between first- and second-order transitions is calculated, and the phase diagrams are presented. Comparing with the results of different directed fields, the qualitative behavior of the phase diagram for the magnetic field along the hard axis is different from the case of the field along the medium axis. For the hard axis the phase boundary lines $k(y)$ shift downwards with increasing h , but upwards for the medium axis. It is shown that the magnetic field along the hard axis favors the occurrence of the first-order transition in the range of parameters under the certain constraint condition. The results can be tested experimentally for molecular magnets Fe_8 and Fe_4 .

DOI: 10.1103/PhysRevB.70.012409

PACS number(s): 75.50.Xx, 75.45.+j, 03.65.Sq

Quantum spin tunneling at low temperatures has attracted considerable attention in view of a possible experimental test of the tunneling effect for mesoscopic single-domain particles. Up until now, molecular magnets are the most promising candidates to observe macroscopic quantum coherence.¹ When the temperature increases the thermal hopping becomes dominant beyond some crossover temperatures. Since the first- and second-order transitions between the quantum and classical behaviors of the escape rates in spin systems were introduced by Chudnovsky and Garanin,^{2,3} a lot of work has been done theoretically and experimentally.^{4–14} Most theoretical studies focus on ferromagnetic particles. It is shown that quantum tunneling occurs at higher temperatures and higher frequencies in antiferromagnetic particles than in ferromagnetic particles of the same size.¹⁵ Strictly speaking, the most so-called ferromagnetic systems are actually ferrimagnetic. So the nanometer-scale antiferromagnets are more interesting from experimental and theoretical aspects. For instance, quantum tunneling on a supramolecular magnet dimer $[\text{Mn}_4]_2$ with the antiferromagnetic coupling between two Mn_4 units was investigated experimentally and theoretically.^{16,17} The strong exchange interaction was also taken into account in the study of quantum-classical crossover of the escape rates.^{18–21} More recently, the quantum-classical crossover in biaxial antiferromagnetic particles in the presence of an external magnetic field along the medium axis or the easy axis was investigated.^{19,20} It is noted that an experimental observation of quantum phase interference, introduced by an external magnetic field along the hard axis for molecular magnet Fe_8 , was reported.¹ Considering that molecular magnet Fe_8 is characterized by a large spin ground state that originates from an incomplete compensation of antiferromagnetically coupled spins,²² and is actually ferrimagnetic, in the study of the quantum-classical crossover of biaxial antiferromagnetic particles, the case of a magnetic field along the hard axis deserves further investigation. In this paper we attempt to investigate the effect of a magnetic field along the hard axis

on the quantum-classical crossover behavior of the escape rate of biaxial antiferromagnetic particles. Comparing with the results of different directed fields, the qualitative behavior of the phase diagram for the magnetic field along the hard axis is different from the case of the field along the medium axis. For the hard axis the phase boundary lines $k(y)$ shift downwards with increasing h , but upwards for the medium axis. It is shown that the magnetic field along the hard axis favors the occurrence of the first-order transition in the range of parameters under the certain constraint condition.

We consider a small biaxial antiferromagnetic particle with two magnetic sublattices whose magnetizations, \mathbf{m}_1 and \mathbf{m}_2 , are coupled by the strong exchange interaction $\mathbf{m}_1 \cdot \mathbf{m}_2 / \chi_\perp$, where χ_\perp is the perpendicular susceptibility. The system has a noncompensation of sublattices with $m(=m_1 - m_2 > 0)$, with the easy axis x , the medium axis y , and the hard axis z . In the presence of a magnetic field along the hard axis, the Euclidean action is written as¹⁵

$$S_E(\theta, \phi) = V \int d\tau \left\{ i \frac{m_1 + m_2}{\gamma} \dot{\phi} - i \frac{m}{\gamma} \dot{\phi} \cos \theta + \frac{\tilde{\chi}_\perp}{2\gamma^2} [\dot{\theta}^2 + (\dot{\phi} - i\gamma H)^2 \sin^2 \theta] + K_1 \cos^2 \theta + K_2 \sin^2 \theta \sin^2 \phi - mH \cos \theta \right\}, \quad (1)$$

where V is the volume of the particle, γ the gyromagnetic ratio, and $\tilde{\chi}_\perp = \chi_\perp (m_2/m_1)$. K_1 and K_2 ($K_1 > K_2$) are the transverse and longitudinal anisotropic coefficients, respectively. The polar coordinate θ and the azimuthal coordinate ϕ for the angular components of \mathbf{m}_1 in the spherical coordinate system determine the direction of the Néel vector. A dot over a symbol denotes a derivative with respect to the Euclidean time τ . The classical trajectory to the Euclidean action (1) is determined by

$$-in\dot{\phi}\sin\theta+x\left(\ddot{\theta}-\frac{1}{2}\dot{\phi}^2\sin 2\theta+ib\dot{\phi}\sin 2\theta\right)-2hk\sin\theta$$

$$+\sin 2\theta(1-k\sin^2\phi)+\frac{1}{2}b^2x\sin 2\theta=0, \quad (2)$$

$$in\dot{\theta}+x(\dot{\phi}\sin\theta+2\dot{\phi}\dot{\theta}\cos\theta-2ib\dot{\theta}\cos\theta)-k\sin\theta\sin 2\phi$$

$$=0, \quad (3)$$

where $n=m/(K_1\gamma)$, $x=\tilde{\chi}_\perp/(K_1\gamma^2)$, $k=K_2/K_1$, $b=\gamma H$, $h=H/H_c$, and $H_c=2K_2/m$.

In the high-temperature regime the sphaleron solution of Eqs. (2) and (3) is $(\theta_0=\arccos h_0, \phi_0=\pi/2)$, where $h_0=hk/(1-k+xb^2/2)\leq 1$. The crossover behavior of the escape rate from the quantum tunneling to the thermal activation is obtained from the deviation of the period of the periodic instanton from that of the sphaleron.^{18,24} To this end we expand (θ, ϕ) about the sphaleron configurations θ_0 and ϕ_0 , i.e., $\theta=\theta_0+\eta(\tau)$ and $\phi=\phi_0+\xi(\tau)$, where $\phi_0=\pi/2$. Denote $\delta\Omega(\tau)\equiv[\eta(\tau), \xi(\tau)]$, at finite temperature $\delta\Omega(\tau+\beta\hbar)=\delta\Omega(\tau)$. Thus it can be expanded in the Fourier series $\delta\Omega(\tau)=\sum_{n=-\infty}^{\infty}\delta\Omega_n\exp[i\omega_n\tau]$, where $\omega_n=2\pi n/\beta\hbar$. To the lowest order $\eta\simeq ia\theta_1\sin(\omega\tau)$ and $\xi\simeq a\phi_1\cos(\omega\tau)$. Here, a serves as a perturbation parameter. Substituting them into Eqs. (2) and (3), and neglecting the terms of order higher than a , we obtain the relation

$$\frac{\phi_1}{\theta_1}=\frac{x\omega_\pm^2+\sin^2\theta_0(2-2k+xb^2)}{\omega_\pm(n\sin\theta_0-bx\sin 2\theta_0)}=-\frac{\omega_\pm(n-2bx\cos\theta_0)}{\sin\theta_0(x\omega_\pm^2-2k)}, \quad (4)$$

and the oscillation frequency

$$\omega_\pm^2=-\frac{1}{2x^2}\{x[\sin^2\theta_0(2-2k+xb^2)-2k]+(n-2xb\cos\theta_0)^2\}$$

$$\pm\frac{1}{2x^2}\{8kx^2(2-2k+xb^2)\sin^2\theta_0$$

$$+[x(\sin^2\theta_0(2-2k+xb^2)-2k)+(n-2xb\cos\theta_0)^2]^2\}^{1/2}. \quad (5)$$

Next, let us write $\eta\simeq ia\theta_1\sin(\omega\tau)+\eta_2$ and $\xi\simeq a\phi_1\cos(\omega\tau)+i\xi_2$, where η_2 and ξ_2 are of the order of a^2 . Inserting them into Eqs. (2) and (3), we arrive at $\omega=\omega_+$ and

$$\eta_2=a^2p_0+a^2p_2\cos(2\omega\tau), \quad (6)$$

$$\xi_2=a^2q_2\sin(2\omega\tau), \quad (7)$$

where the analytic forms of coefficients p_0 , p_2 , and q_2 are listed in the Appendix. It implies that there is no shift in the oscillation frequency. In order to find the change of the oscillation period, we proceed to the third order of perturbation theory by writing $\eta\simeq ia\theta_1\sin(\omega\tau)+\eta_2+i\eta_3$, and $\xi\simeq a\phi_1\cos(\omega\tau)+i\xi_2+\xi_3$, where η_3 and ξ_3 are of the order a^3 . Substituting them again into Eqs. (2) and (3), and keeping the terms up to $O(a^3)$, we yield equations to determine η_3 , ξ_3 and the corresponding frequency ω . After some tedious algebra we obtain

$$\eta_3=a^3p_3\sin(3\omega\tau), \quad \xi_3=a^3q_3\cos(3\omega\tau), \quad (8)$$

where the analytic forms of real coefficients p_3 and q_3 are cumbersome, and are not listed in the paper. We also have

$$n^4y^2(\omega^2-\omega_+^2)(\omega^2-\omega_-^2)=a^2\frac{\phi_1^2}{4}g(h,k,y), \quad (9)$$

where

$$g(h,k,y)=g_1(h,k,y)+g_2(h,k,y), \quad (10)$$

and $y=x/n^2(=\tilde{\chi}_\perp K_1/m^2)$. The forms of $g_1(h,k,y)$ and $g_2(h,k,y)$ are given by

$$g_1(h,k,y)=(1-4hky\cos\theta_0)w\left\{\frac{2}{\lambda^2}hkyw\cos\theta_0\right.$$

$$+\frac{\sin\theta_0}{\lambda}\left(k-\frac{5}{2}yw^2\right)$$

$$-4\tilde{q}_2k\cos\theta_0-8(2\tilde{p}_0-\tilde{p}_2)hkyw\sin\theta_0$$

$$+4\lambda\left[(2\tilde{p}_0+\tilde{p}_2)k\cos\theta_0-k\sin\theta_0\right.$$

$$\left.-\left(\tilde{p}_0-\frac{3}{2}\tilde{p}_2\right)yw^2\cos\theta_0\right\}, \quad (11)$$

$$g_2(h,k,y)=-\frac{(1-4hky\cos\theta_0)w}{\sin\theta_0}\left\{\frac{1}{\lambda^3}[-hk\cos\theta_0\right.$$

$$+4(1-k+2h^2k^2y)\cos 2\theta_0]$$

$$+\frac{12w}{\lambda^2}\left(\frac{1}{8}\sin\theta_0-hky\sin 2\theta_0\right)$$

$$+\frac{4}{\lambda}\left[\left(\frac{1}{2}k+4hkyw\tilde{q}_2-\frac{3}{4}yw^2\right)\cos 2\theta_0\right.$$

$$+(2\tilde{p}_0-\tilde{p}_2)hk\sin\theta_0-\tilde{q}_2w\cos\theta_0$$

$$-2(2\tilde{p}_0-\tilde{p}_2)\sin 2\theta_0(1-k+2h^2k^2y)]$$

$$+4(k-yw^2)\tilde{q}_2\sin 2\theta_0+2(2\tilde{p}_0-\tilde{p}_2)w\cos\theta_0$$

$$\left.-8(2\tilde{p}_0-\tilde{p}_2)hkyw\cos 2\theta_0\right\}, \quad (12)$$

where $w=n\omega_+$ and $\lambda=\phi_1/\theta_1$. The parameter $y=x/n^2(=\tilde{\chi}_\perp K_1/m^2)$ indicates the relative magnitude of the noncompensation. For a large noncompensation ($y\ll 1$, i.e., $m\gg\sqrt{\tilde{\chi}_\perp K_1}$) the system becomes ferromagnetic, while for a small noncompensation ($y\gg 1$, i.e., $m\ll\sqrt{\tilde{\chi}_\perp K_1}$) the system becomes nearly compensated antiferromagnetic.¹⁸ Also, \tilde{p}_0 , \tilde{p}_2 , and \tilde{q}_2 are obtained by replacing θ_1 by ϕ_1/λ and dropping ϕ_1^2 in p_0 , p_2 , and q_2 , respectively. It is shown that for $h=0$, Eq. (10) is reduced to Eq. (17) in Ref. 18.

According to the theory by Chudnovsky,²³ the order of quantum-classical crossover is determined by the behavior of the Euclidean time oscillation period $\tau(E)$, where E is the energy near the bottom of the Euclidean potential. The existence of a minimum in the oscillation period with respect to

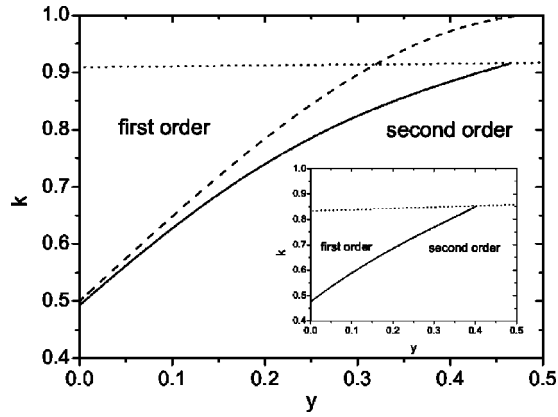


FIG. 1. Phase diagram $k(y)$. The solid line corresponds to $h = 0.1$ and the dashed line to $h = 0$. The dotted line is determined by the constraint condition $h_0 \leq 1$ [i.e., $hk/(1-k+2h^2k^2y) \leq 1$]. The inset corresponds to $h = 0.2$.

energy, i.e., in the $\tau \sim E$ curve, was proposed as a criteria for first-order transition. Thus, the period $\tau (=2\pi/\omega)$ in Eq. (9) should be less than $\tau_+ (=2\pi/\omega_+)$, i.e., $\omega > \omega_+$ for the first-order transition. It implies that $g(h, k, y) > 0$ in Eq. (9), and $g(h, k, y) = 0$ determines the phase boundary between the first- and the second-order transition. We first solve Eq. (9) numerically to obtain the phase boundary lines $k(y)$'s for several values of h , which are plotted in Fig. 1, where the constraint condition $h_0 \leq 1$ [i.e., $hk/(1-k+2h^2k^2y) \leq 1$] has been considered. Figure 1 shows that the phase boundary lines $k(y)$ shift downwards with increasing h . For instance, in the case of $y = 0.25$ the first-order transition vanishes for $k = 0.844, 0.785, 0.728$, and $h = 0.0, 0.1, 0.2$, respectively. It is also interesting to consider the limit case of $y \rightarrow 0$. The case corresponds to biaxial ferromagnetic particles. Note that the quantum-classical crossover for biaxial ferromagnetic particles in the presence of an external magnetic field along the hard axis was investigated in Ref. 10. From Fig. 1 in the limit case of $y \rightarrow 0$, the first-order transition vanishes for $k = 0.5, 0.493, 0.476$, and $h = 0.0, 0.1, 0.2$, respectively. The results agree with those obtained from Eq. (19) in Ref. 10 (note that h defined in Ref. 10 corresponds to hk here). Comparing with the results of different directed fields^{19,20} (see Fig. 2), the qualitative behavior of the phase diagram for the magnetic field along the hard axis is different from the case of the field along the medium axis, in which the phase boundary line $k(y)$ shifts upwards with increasing h . Figure 2 shows that in the range of parameters under the constraint condition $h_0 \leq 1$, the magnetic field along the hard axis favors the occurrence of the first-order transition. For instance, in the case of $h = 0.1$ and $k = 0.85$ the first-order transition vanishes beyond $y = 0.138, 0.261$, and 0.335 for the field along the medium axis, easy axis, and hard axis, respectively. To illustrate the above results with concrete examples, firstly we discuss the molecular magnet Fe_8 , which is actually ferromagnetic, and thereby y should be taken into account in the biaxial symmetry. Take the measured value of the anisotropy parameter, e.g., $k = 0.728$ for Fe_8 .¹ The phase boundary line $h(y)$ for $k = 0.728$ is shown in Fig. 3 (dashed line). For Fe_8 the maximum of the critical value y_c , beyond which the first-

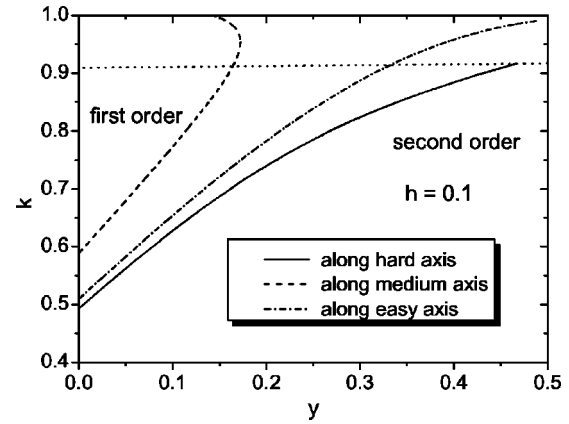


FIG. 2. Phase diagram $k(y)$ for different directed fields with $h = 0.1$. The solid line corresponds to field along the hard axis, the dashed line to field along the medium axis, and the dashed-dotted line to field along the easy axis. The dashed and dashed-dotted lines are plotted according to Refs. 19 and 20. The dotted line is determined by the constraint condition $hk/(1-k+2h^2k^2y) \leq 1$ for field along the hard axis.

order transition vanishes, is about 0.313. Next we consider molecular magnet $\text{Fe}_4(\text{OCH}_3)_6(\text{dpm})_6$, Fe_4 for simplicity, as another example. The cluster Fe_4 is characterized by an $S = 5$ ground state arising from antiferromagnetic interaction between central and peripheral iron spins.²⁵⁻²⁸ According to the estimate of the transverse and longitudinal anisotropic coefficients for Fe_4 in Refs. 25-28, $k = 0.822$. The phase boundary line $h(y)$ for $k = 0.822$ is also shown in Fig. 3 (solid line). For Fe_4 the maximum of the critical value y_c is about 0.378.

In conclusion, the quantum-classical crossover of the escape rate for biaxial antiferromagnetic particles is investigated in the presence of a magnetic field along the hard axis. The nonlinear perturbation method is applied to establish the phase diagrams for first- and second-order transitions. Comparing with the results of different directed fields, it shows that in the range of parameters under the constraint condition $h_0 \leq 1$, the magnetic field along the hard axis favors the oc-

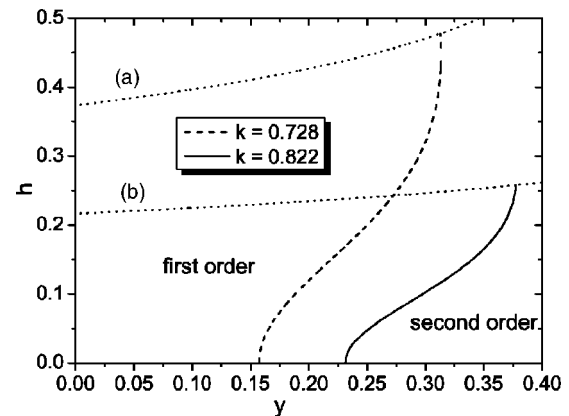


FIG. 3. Phase diagram for the orders of transition in the (y, h) plane in Fe_8 ($k = 0.728$) and Fe_4 ($k = 0.822$). The dotted line (a) determined by the constraint condition $hk/(1-k+2h^2k^2y) \leq 1$ corresponds to the case of Fe_8 , and the dotted line (b) to Fe_4 .

currence of the first-order transition. Two cases of the molecular magnets Fe_8 and Fe_4 are also investigated.

B.Z. acknowledges the support of the China Postdoctoral Science Foundation (No. 2002032138) and the National Natural Science Foundation of China (No. 10347106). R.T. acknowledges the support of the National Natural Science Foundation of China (Nos. 10174015 and 10234010) and the 973 Project of China (No. 2002CB613504). S-Q.S. acknowledges the support of the Research Grants Council of Hong Kong (No. HKU7023/03P).

APPENDIX

The coefficients in Eqs. (6) and (7) are listed as follows:

$$p_0 = \{2bx\omega\theta_1\phi_1 \cos 2\theta_0 - hk\theta_1^2 \sin \theta_0 + (2 - 2k + b^2x)\theta_1^2 \sin 2\theta_0 + \left(k - \frac{x\omega_+^2}{2}\right)\phi_1^2 \sin 2\theta_0 - n\omega\theta_1\phi_1 \cos \theta_0\} / \{2 \sin^2 \theta_0 (2 - 2k + b^2x)\},$$

$$p_2 = - \left\{ hk(k - 2x\omega^2)\theta_1^2 \sin \theta_0 + 2bx\omega(k\theta_1\phi_1 + n\omega\theta_1^2 \sin \theta_0 - 2x\omega^2\theta_1\phi_1) + 2bx^2\omega(4\omega^2 - 3\omega_+^2)\theta_1\phi_1 \cos^2 \theta_0 + k^2(2\theta_1^2 + \phi_1^2)\sin 2\theta_0 - nk\omega\theta_1\phi_1 \cos \theta_0 - k(2 + b^2x + 4x\omega^2)\theta_1^2 \sin 2\theta_0 - \frac{1}{2}kx\phi_1^2(4\omega^2 - \omega_+^2)\sin 2\theta_0 + 4x\omega^2\theta_1^2 \sin 2\theta_0 - nx\omega\theta_1\phi_1(2\omega^2 - 3\omega_+^2)\cos \theta_0 - x^2\omega^2\omega_+^2\phi_1^2 \sin 2\theta_0 \right\} / \{-4(h \cos \theta_0 + \cos 2\theta_0)k^2 + 2k[4hx\omega^2 \cos \theta_0 + 2 \cos^2 \theta_0(2 + b^2x + 4x\omega^2) - 2 - b^2x - 8x\omega^2] + 4\omega^2[n^2 - 4nbx \cos \theta_0 + 2x + b^2x^2 + 4x^2\omega^2 - 2x \cos^2 \theta_0(2 - b^2x)]\},$$

$$q_2 = \{2\theta_1\omega[2nbx\omega\phi_1 + \theta_1(2 - 2k + b^2x + 4x\omega^2)bx \sin \theta_0 + hkn\theta_1 \sin \theta_0] - 2\theta_1\phi_1 \cos^3 \theta_0[4k^2 - 2k(2 + b^2x + 3x\omega_+^2) + 6x\omega_+^2 + b^2x^2(-8\omega^2 + 3\omega_+^2)] - 2 \cos^2 \theta_0[hk\theta_1\phi_1(2k - 3x\omega_+^2) + 2bx\omega((-2 + 2k - b^2x)\theta_1^2 \sin \theta_0 + 3n\omega\theta_1\phi_1 + (2k + x\omega_+^2)\phi_1^2 \sin \theta_0)] + \cos \theta_0[4k^2\theta_1\phi_1 + 2n^2\omega^2\theta_1\phi_1 - 2n\omega \sin \theta_0(2(2 + b^2x)\theta_1^2 - x\omega_+^2\phi_1^2) + x\theta_1\phi_1(6(1 + 2x\omega^2)\omega_+^2 + b^2x(-8\omega^2 + 3\omega_+^2)) + 2k(4n\omega\theta_1^2 \sin \theta_0 + 2n\omega\phi_1^2 \sin \theta_0 - \theta_1\phi_1(2 + b^2x + 4x\omega^2 + 3x\omega_+^2))]\} / \{4 \sin \theta_0[2(h \cos \theta_0 + \cos 2\theta_0)k^2 + k(8x\omega^2 \sin^2 \theta_0 - 4hx\omega^2 \cos \theta_0 - \cos 2\theta_0(2 + b^2x)) - 2\omega^2(n^2 - 4nbx \cos \theta_0 + 2x + b^2x^2 + 4x^2\omega^2 - 2x \cos^2 \theta_0(2 - b^2x))]\}.$$

¹W. Wernsderfer and R. Sessoli, *Science* **284**, 133 (1999).
²E.M. Chudnovsky and D.A. Garanin, *Phys. Rev. Lett.* **79**, 4469 (1997).
³D.A. Garanin and E.M. Chudnovsky, *Phys. Rev. B* **56**, 11102 (1997).
⁴H.J.W. Müller-Kirsten *et al.*, *Phys. Rev. B* **60**, 6662 (1999).
⁵J.-Q. Liang *et al.*, *Phys. Rev. Lett.* **81**, 216 (1998).
⁶G.-H. Kim, *Phys. Rev. B* **59**, 11847 (1999).
⁷G.-H. Kim and E.M. Chudnovsky, *Europhys. Lett.* **52**, 681 (2000).
⁸D.A. Garanin *et al.*, *Phys. Rev. B* **57**, 13639 (1998).
⁹D.A. Garanin and E.M. Chudnovsky, *Phys. Rev. B* **59**, 3671 (1999).
¹⁰X. Martínez Hidalgo and E.M. Chudnovsky, *J. Phys.: Condens. Matter* **12**, 4243 (2000).
¹¹B. Zhou *et al.*, *Physica B* **301**, 180 (2001).
¹²S.Y. Lee *et al.*, *Phys. Rev. B* **58**, 5554 (1998).
¹³A.D. Kent *et al.*, *Europhys. Lett.* **49**, 521 (2000).
¹⁴L. Bokacheva, A.D. Kent, and M.A. Walters, *Phys. Rev. Lett.* **85**, 4803 (2000).

¹⁵E.M. Chudnovsky, *J. Magn. Magn. Mater.* **140**, 1821 (1995); B. Barbara, and E.M. Chudnovsky, *Phys. Lett. A* **145**, 205 (1990).
¹⁶W. Wernsderfer *et al.*, *Nature (London)* **416**, 406 (2002).
¹⁷K. Park *et al.*, *Phys. Rev. B* **68**, 020405 (2003); G.-H. Kim, *ibid.* **67**, 024421 (2003); J.M. Hu, Z.D. Chen, and S.-Q. Shen, *ibid.* **68**, 104407 (2003); Y. Su and R. Tao, *ibid.* **68**, 024431 (2003).
¹⁸G.-H. Kim, *Europhys. Lett.* **51**, 216 (2000).
¹⁹B. Zhou *et al.*, *Phys. Rev. B* **64**, 132407 (2001).
²⁰G.-H. Kim, *Phys. Rev. B* **67**, 144413 (2003).
²¹B. Zhou *et al.*, *Phys. Rev. B* **68**, 214423 (2003).
²²A. Caneschi *et al.*, *J. Magn. Magn. Mater.* **200**, 182 (1999).
²³E.M. Chudnovsky, *Phys. Rev. A* **46**, 8011 (1992).
²⁴D.A. Gorokhov and G. Blatter, *Phys. Rev. B* **56**, 3130 (1997).
²⁵A.L. Barra *et al.*, *J. Am. Chem. Soc.* **121**, 5302 (1999).
²⁶A. Bouwen *et al.*, *J. Phys. Chem. B* **105**, 2658 (2001).
²⁷G. Amoretti *et al.*, *Phys. Rev. B* **64**, 104403 (2001).
²⁸T.J. Burns and J. Oitmaa, *Europhys. Lett.* **63**, 764 (2003).